

Optical absorption spectra of tripositive erbium ion in certain nitrate complexes

S V J LAKSHMAN and C K JAYASANKAR

Department of Physics, S V University, Tirupati 517 502, India

MS received 16 November 1983; revised 7 May 1984

Abstract. Optical absorption of Er^{3+} ion in $\text{Er}(\text{NO}_3)_3 \cdot 5\text{H}_2\text{O}$, NH_4NO_3 , $\text{Mg}(\text{NO}_3)_2 \cdot 6\text{H}_2\text{O}$, KNO_3 and NaNO_3 complexes has been studied. The second derivative spectra of these Er^{3+} complexes exhibited splittings in the $^4I_{9/2}$, $^4F_{9/2}$, $^4F_{7/2}$, $^4F_{5/2}$ and $^2H_{9/2}$ levels. These splittings have been tentatively explained as due to a cubic crystalline field. The partial derivatives for Er^{3+} ion have been calculated in terms of Racah (E^k) parameters. The results of a least squares fit of the energy levels and oscillator strengths of the bands are reported in terms of interaction parameters and Judd-Ofelt parameters. Radiative transition probabilities for various fluorescence levels are theoretically estimated. The lifetime of the $^4G_{11,2}$ level is found to be lowest in all nitrate complexes.

Keywords. Erbium nitrate; optical absorption; oscillator strengths; transition probability; derivative spectrum; tripositive erbium.

PACS No. 78-50

1. Introduction

Considerable progress has been made in interpreting the optical spectra of Er^{3+} ion embedded in crystalline solids (Dieke 1968; Hufner 1978; Wybourn 1965; Crosswhite and Moos 1967; Chang *et al* 1982; Gruber *et al* 1982; Hayhurst *et al* 1981; Ryba-Romanowski *et al* 1980; Faulkner *et al* 1980; Mazurak *et al* 1983), in different solution media (Carnall *et al* 1965, 1968; Hoogschagen and Gorter 1948; Lakshman and Jayasankar 1984), in glasses (Reisfeld and Eckstein 1975) and in garnets (Pappalardo 1963; Koningstein and Geusic 1964).

Prandtl and Scheiner (1934) presented almost a complete collection of trivalent lanthanide solution absorption spectra. Carnall *et al* (1965) reported the absorption spectra of the trivalent lanthanides in aqueous, acid and molten solutions and correlated the experimentally observed energies and intensities with the corresponding theoretically calculated values. Krupke and Gruber (1963) reported the absorption and fluorescence spectra of Er^{3+} : LaF_3 .

The theoretical interpretation of solution spectra has undergone significant advances in recent years. It is now possible to compute both the energies and intensities of bands. Optical absorption spectra of $\text{Er}(\text{NO}_3)_3 \cdot 5\text{H}_2\text{O}$ in the presence of NH_4NO_3 , $\text{Mg}(\text{NO}_3)_2 \cdot 6\text{H}_2\text{O}$, KNO_3 and NaNO_3 complexes have so far not been reported in literature. The authors therefore recorded both the normal and second derivative spectra of these complexes.

2. Experimental

Saturated solutions of ammonium nitrate (AN), magnesium nitrate (MN), potassium nitrate (PN) and sodium nitrate (SN) were prepared. To each of these solutions 0.1 mole % of 4N erbium nitrate (EN) (M/s Rare Earth Products Limited, London) was added. The absorption spectra of erbium nitrate complexes were recorded in the UV-vis region (45000 cm^{-1} to 12000 cm^{-1}) on a Perkin-Elmer 551 recording spectrophotometer. The second derivative spectra of these complexes were also recorded in this spectral region. The IR spectra in the region from 13000 to 3000 cm^{-1} and 4000 to 200 cm^{-1} for EN in KBr were recorded using Carl-Zeiss Specord 61 and Pye Unicam SP3 300 IR spectrophotometers respectively. The refractive indices of the EN complexes were measured on a PZO RL Nr3275 refractometer. The experimental intensities of the bands were determined from their profiles.

3. Results and analysis

The normal and second derivative spectra of Er^{3+} in EN, AN, MN, PN and SN solutions are shown in figures 1a to 5a and 1b to 5b respectively. The normal spectra closely resemble the spectrum of erbium aquo ion (Carnall 1979). However, the second derivative spectra (figures 1b to 5b) exhibited certain structural details, such as resolution in closely lying high energy (above 25000 cm^{-1}) bands and splitting of low energy bands

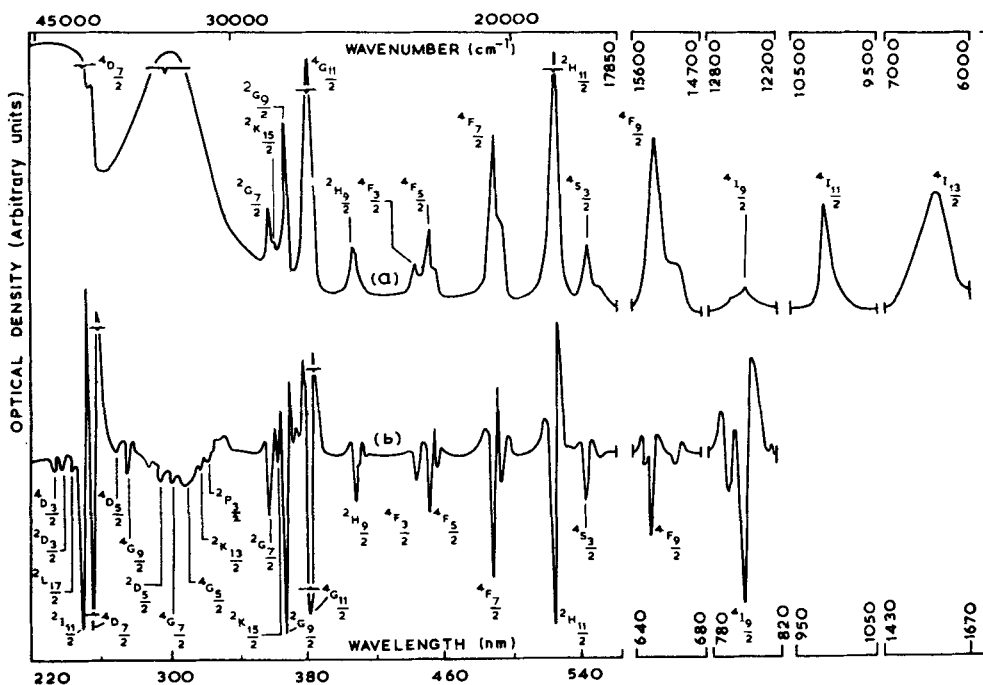


Figure 1. Absorption spectrum of erbium nitrate solution: (a) normal spectrum (b) second derivative spectrum.

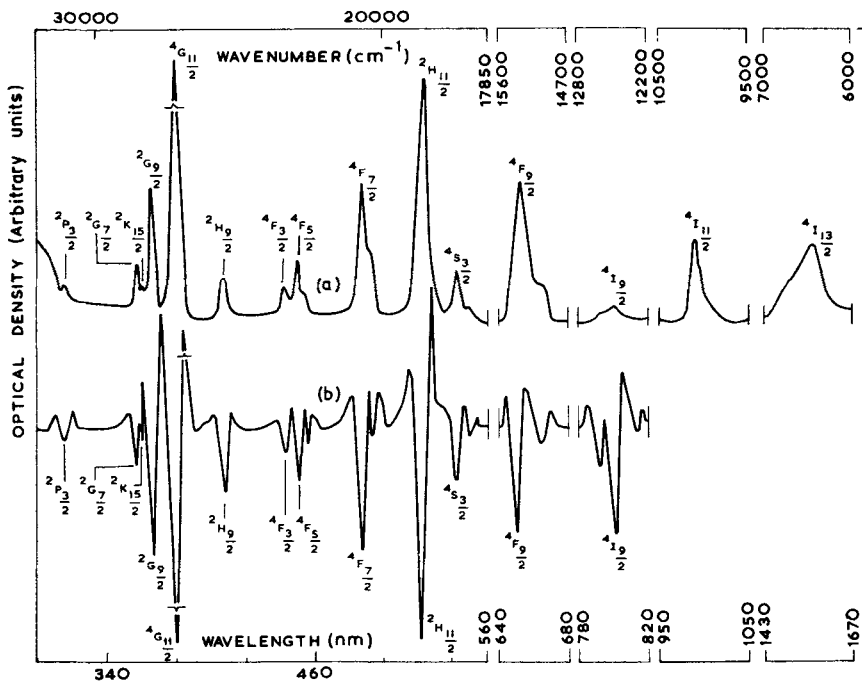


Figure 2. Absorption spectrum of $\text{Er}^{3+}:\text{NH}_4\text{NO}_3$: (a) normal spectrum (b) second derivative spectrum.

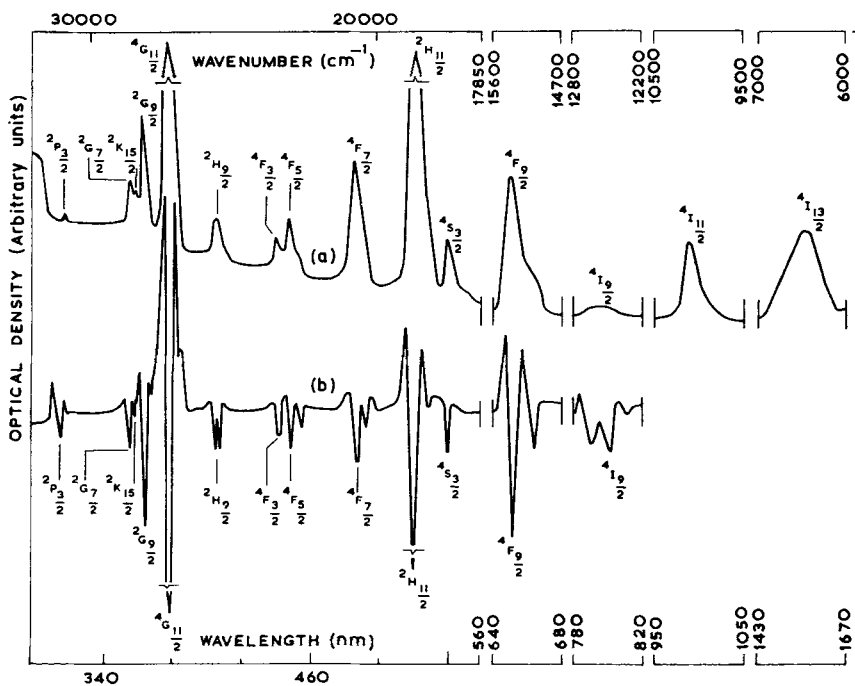


Figure 3. Absorption spectrum of $\text{Er}^{3+}:\text{Mg}(\text{NO}_3)_2 \cdot 6\text{H}_2\text{O}$: (a) normal spectrum (b) second derivative spectrum.

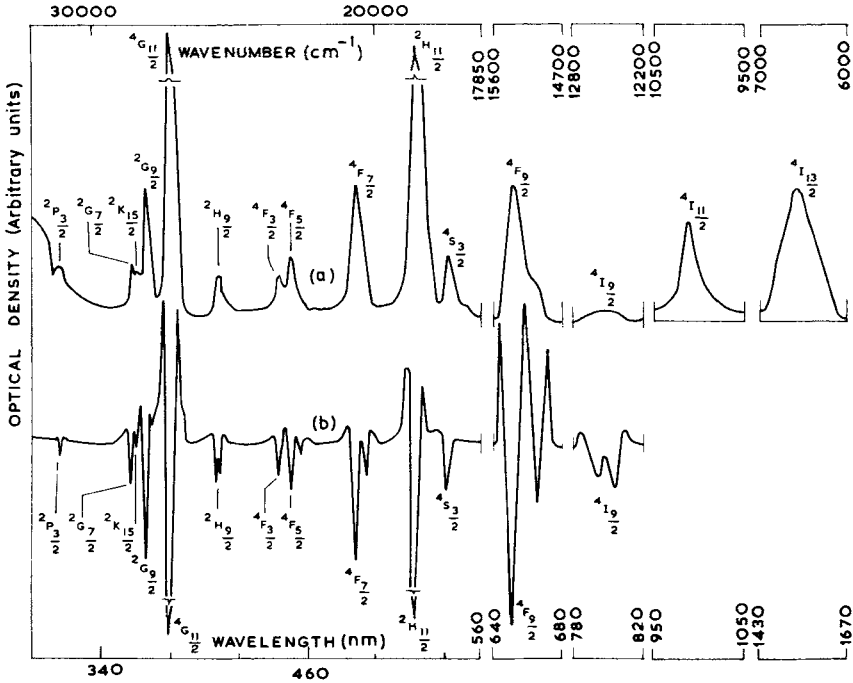


Figure 4. Absorption spectrum of $\text{Er}^{3+}:\text{KNO}_3$: (a) normal spectrum (b) second derivative spectrum.

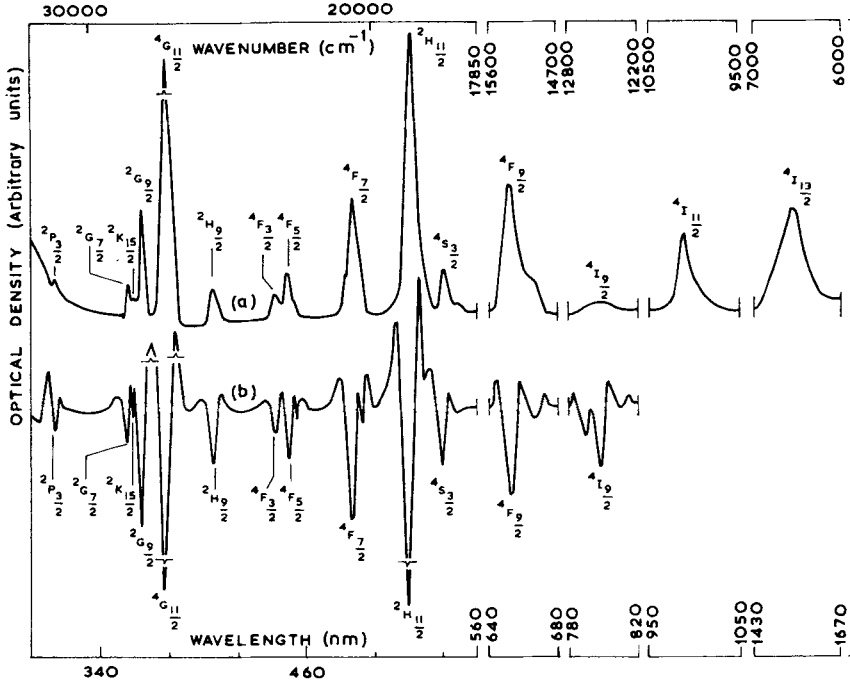


Figure 5. Absorption spectrum of $\text{Er}^{3+}:\text{NaNO}_3$: (a) normal spectrum (b) second derivative spectrum.

and permitted the identification of high energy bands (${}^2K_{15/2}$, ${}^2P_{3/2}$, ${}^4G_{5/2}$, ${}^4G_{7/2}$ etc.,) with certainty.

3.1 Electronic energy levels

The identification and analysis of the bands were straightforward. The wavenumbers of the observed bands are presented in table 1 along with their assignments. Under the influence of the electric field of the solution matrix, the changes in the electrostatic (E^1 , E^2 , E^3), spin-orbit (ξ_{4f}) and configuration interaction (α , β , γ) parameters are very small. To a first order approximation, the energy E_J of the J th level may be expressed in terms of the changes in the parameters P_k ($P_1 = E^1$, $P_2 = E^2$, $P_3 = E^3$, $P_4 = \xi_{4f}$, $P_5 = \alpha$, $P_6 = \beta$ and $P_7 = \gamma$) by a Taylor-series expansion as follows (Wong 1961).

$$E_J = E_{0J} + \sum_{k=1}^7 (dE_J/dP_k) \Delta P_k. \quad (1)$$

E_{0J} is the zero order energy of the level J and dE_J/dP_k are the partial derivatives. Further

$$\Delta P_k = P_k - P_k^0, \quad (2)$$

where P_k^0 is the free ion parameter and P_k is the parameter of the ion in the crystal or solution matrix.

Using the E_{0J} values and the partial derivatives given earlier (Lakshman and Jayasankar 1984) and the experimental band positions as E_J (table 1) for the respective energy levels, (1) was solved by the least squares fit method to evaluate ΔP_k values. From

Table 1. Experimental energy levels (E) and oscillator strengths (f) of Er^{3+} ion in EN, AN, MN, PN, PN and SN nitrate complexes.

Terms	EN		AN		MN		PN		SN	
	E (cm^{-1})	f ($\times 10^{-6}$)	E (cm^{-1})	f ($\times 10^{-6}$)	E (cm^{-1})	f ($\times 10^{-6}$)	E (cm^{-1})	f ($\times 10^{-6}$)	E (cm^{-1})	f ($\times 10^{-6}$)
${}^4I_{13/2}$	6390	—	6615	—	6450	—	6440	—	6560	—
${}^4I_{11/2}$	10115	—	10110	—	10100	—	10105	—	10100	—
${}^4I_{9/2}$	12465	0.187	12497	0.142	12512	0.121	12481	0.110	12489	0.117
${}^4F_{9/2}$	15321	1.656	15338	1.566	15357	1.643	15333	1.308	15338	1.531
${}^4S_{3/2}$	18428	0.322	18496	0.342	18513	0.465	18462	0.355	18507	0.352
${}^2H_{11/2}$	19097	2.419	19189	4.482	19207	4.690	19115	2.417	19196	3.374
${}^4F_{7/2}$	20507	1.292	20528	2.032	20549	1.879	20528	1.152	20537	1.764
${}^4F_{5/2}$	22167	0.471	22265	0.627	22315	0.632	22256	0.474	22241	0.475
${}^4F_{3/2}$	22593	0.255	22644	0.327	22695	0.437	22659	0.262	22644	0.245
${}^2H_{9/2}$	24624	0.606	24533	0.579	24593	0.742	24684	0.530	24624	0.571
${}^4G_{11/2}$	26274	4.793	26343	10.222	26378	11.311	26308	4.268	26364	7.498
${}^2G_{9/2}$	27389	—	27389	—	27465	—	27427	—	27450	—
${}^2K_{15/2}$	27731	—	27770	—	27808	—	27847	—	27785	—
${}^2G_{7/2}$	27964	0.499	28042	0.373	28082	0.349	27886	0.490	28042	0.405
${}^2P_{3/2}$	—	—	31586	—	31662	—	31656	—	31656	—
RMS deviation*	± 89	± 0.202	± 90	± 0.499	± 81	± 0.526	± 94	± 0.274	± 74	± 0.350

* To save space calculated values are not given.

Table 2. Slater-Condon, Racah, spin-orbit, configuration interaction, operator equivalent factors and crystal field parameters of Er^{3+} ion in nitrate complexes (Values in cm^{-1}).

Parameter	EN	AN	MN	PN	SN
F_2	442-737	458-667	452-220	429-060	446-798
F_4	71-176	75-546	72-946	63-583	71-433
F_6	7-589	8-868	8-196	6-319	7-892
E^1	6958-4	7479-0	7212-7	6374-8	7064-0
E^2	31-370	32-678	32-306	31-394	31-971
E^3	650-06	646-55	650-98	650-58	648-15
ζ_{4f}	2386-3	2417-4	2396-0	2401-3	2407-6
α	22-343	23-573	22-564	26-265	22-288
β	-859-82	-926-90	-876-08	-1016-28	-872-51
γ	-273-22	-2574-37	-1264-81	2836-75	-625-21
$\beta_J \times 10^5$	4-5113	4-5131	4-5115	4-5117	4-5124
$\gamma_J \times 10^6$	2-0020	2-0000	2-0020	2-0020	2-0010
A_{40}	-127-4	-111-4	-107-5	-130-6	-125-8
A_{60}	78-8	91-4	99-8	84-1	95-5

these delta values, the parameters E^1 , E^2 , E^3 , ζ_{4f} , α , β , and γ for Er^{3+} in EN, AN, MN, PN and SN complexes were calculated using (2) and are presented in table 2.

The RMS deviations ± 89 , ± 90 , ± 81 , ± 94 and $\pm 74 \text{ cm}^{-1}$ in EN, AN, MN, PN and SN complexes (table 1) are quite encouraging. The interelectronic repulsion, spin-orbit and configuration interaction parameters now obtained for Er^{3+} in AN, MN, PN and SN along with the EN are also given in table 2. It is interesting that the hydrogenic ratios F_4/F_2 and F_6/F_2 ratios are each equal to 0-161 and 0-017 respectively for the Er^{3+} in EN and are almost the same for the ion in different environments. This suggests that although the environment matrix changes from system to system, the radial properties of the tripositive erbium ion remain unaffected.

3.2 Spectral intensities

The oscillator strength (f) is expressed as

$$f = 4.318 \times 10^{-9} \int \epsilon(\nu) d\nu, \quad (3)$$

where $\epsilon(\nu)$ is the molar extinction coefficient corresponding to the energy of the transition ν . The molar absorptivity at a given energy is computed from the Beer-Lambert law

$$\epsilon = (1/Cl) \log (I_0/I), \quad (4)$$

where C is the concentration of the substance in moles/litre, l is the light path in the solution (cm) and $\log (I_0/I)$ is the absorptivity or optical density which is directly read from the instrument. $d\nu$ is the bandwidth at half height at energy ν .

The observed oscillator strengths, calculated using Judd-Ofelt theory (Carnall *et al* 1965), for Er^{3+} ion in EN, AN, MN, PN and SN complexes are presented in table 1. The small RMS deviations obtained between the observed and calculated values (table 1) support the validity of the Judd-Ofelt theory. The refractive indices (n) and the Judd-Ofelt intensity parameters T_λ and Ω_λ for the complexes studied are presented in table 3.

Table 3. Refractive index (n) and Judd-Ofelt intensity parameters (T_2 and Ω_2) for Er^{3+} ion in different nitrate complexes.

	Complex				
	$\text{Er}^{3+}:\text{Er}(\text{NO}_3)_3 \cdot 5\text{H}_2\text{O}$	$\text{Er}^{3+}:\text{NH}_4\text{NO}_3$	$\text{Er}^{3+}:\text{Mg}(\text{NO}_3)_2 \cdot 6\text{H}_2\text{O}$	$\text{Er}^{3+}:\text{KNO}_3$	$\text{Er}^{3+}:\text{NaNO}_3$
n	1.3362	1.4117	1.4008	1.3602	1.3883
$T_2 \times 10^9$	0.0709	0.2815	0.3089	0.0868	0.1807
$T_4 \times 10^9$	0.1961	0.1624	0.1732	0.1466	0.1654
$T_6 \times 10^9$	0.0490	0.0927	0.0878	0.0511	0.0763
$\Omega_2 \times 10^{20}$ (cm^2)	0.8774	3.3081	3.6580	1.0571	2.1586
$\Omega_4 \times 10^{20}$ (cm^2)	2.4269	1.9085	2.0510	1.7853	1.9758
$\Omega_6 \times 10^{20}$ (cm^2)	0.6064	1.0894	1.0397	0.6223	0.9115

3.3 Hypersensitive transitions

For Er^{3+} ion, ${}^4I_{15/2} \rightarrow {}^2H_{11/2}$ and ${}^4I_{15/2} \rightarrow {}^4G_{11/2}$ transitions are the hypersensitive transitions (Peacock 1975). The oscillator strengths and intensity parameter (T_2) of these transitions are as follows:

Complex	$T_2 \times 10^9$	$f \times 10^6$	
		${}^4I_{15/2} \rightarrow {}^2H_{11/2}$	${}^4I_{15/2} \rightarrow {}^4G_{11/2}$
MN	0.3089	4.690	11.311
AN	0.2815	4.482	10.222
SN	0.1807	3.374	7.498
PN	0.0868	2.457	4.968
EN	0.0709	2.419	4.793

As can be seen, the oscillator strengths of these hypersensitive transitions decrease with the decrease of T_2 parameter which is in accordance with the theory (Peacock 1975). The intensities of these hypersensitive transitions are highest in MN indicating greater involvement of the f orbitals of Er^{3+} ion in MN than in the other complexes.

3.4 Radiative lifetimes

Stein and Wurzburg (1975) pointed out that ${}^4F_{9/2}$ is the highest non-fluorescent level and ${}^4S_{3/2}$ is the lowest fluorescent level in perchlorate solution of Er^{3+} . Radiative lifetimes for ${}^4I_{13/2}$, ${}^4I_{11/2}$, ${}^4I_{9/2}$, ${}^4F_{9/2}$, ${}^4S_{3/2}$, ${}^4F_{7/2}$, ${}^4F_{5/2}$, ${}^2H_{9/2}$ and ${}^4G_{11/2}$ excited states have been theoretically evaluated (Reisfeld 1975; Lakshman and Jayasankar 1984) and presented in table 4.

It is interesting that the lifetime of the ${}^4G_{11/2}$ level is least in all complexes and ${}^4I_{11/2}$ level is highest in EN, AN, PN and SN while that of ${}^4I_{13/2}$ is highest in MN. This clearly reveals that the lifetime of each fluorescent level behaves differently in different environments. For example, the lifetime of the ${}^4S_{3/2}$ is highest in EN and least in AN, whereas that of ${}^4F_{9/2}$ is highest in PN and least in MN. The lifetime variations found for the different levels in different environments are as follows:

$${}^4G_{11/2} : \text{PN} > \text{EN} > \text{SN} > \text{AN} > \text{MN},$$

$${}^2H_{9/2} : \text{PN} > \text{EN} > \text{SN} > \text{MN} > \text{AN},$$

$${}^4F_{5/2} : \text{PN} > \text{EN} > \text{SN} > \text{MN} > \text{AN},$$

$${}^4F_{7/2} : \text{PN} > \text{EN} > \text{SN} > \text{MN} > \text{AN},$$

$${}^4S_{3/2} : \text{EN} > \text{PN} > \text{SN} > \text{MN} > \text{AN},$$

$${}^4F_{9/2} : \text{PN} > \text{EN} > \text{SN} > \text{AN} > \text{MN},$$

$${}^4I_{9/2} : \text{PN} > \text{EN} > \text{SN} > \text{MN} > \text{AN}.$$

$${}^4I_{11/2} : \text{EN} > \text{PN} > \text{SN} > \text{MN} > \text{AN},$$

$${}^4I_{13/2} : \text{EN} > \text{PN} > \text{SN} > \text{MN} > \text{AN}.$$

4. Discussion

The normal spectrum for Er^{3+} in EN in figure 1a exhibits two broad bands at 33000 cm^{-1} and 42000 cm^{-1} . These bands exhibited structural details in the second derivative spectrum as shown in figure 1b. From the theoretically evaluated band positions, the resolved components of high energy bands (in the second derivative spectrum) have been identified as electronic levels. These are presented in table 5.

The absorption spectrum of EN is recorded in the wavenumber region of 45000 cm^{-1} to 3000 cm^{-1} . However, the spectra of Er^{3+} in AN, MN, PN and SN were recorded only up to 32000 cm^{-1} since beyond this region no bands could be observed due to abnormal noise. Carnall *et al* (1965) also made similar observation in the nitrate complexes.

The second derivative spectra (figures 1b to 5b) showed splittings for some low energy bands. They may be due to (a) impurity (b) another ionic species (c) superposition of vibronic modes of ligands on electronic levels or (d) crystal (ligand) field. Since a very pure form of erbium nitrate is used and the hosts are also analar samples (99.99%), the first possibility is ruled out. The second possibility is also ruled out as the erbium atom is not stable in any ionic state other than Er^{3+} (Dieke 1968;

Table 4. Predicted lifetimes for the fluorescent levels of Er^{3+} ion in certain nitrate complexes (Values in μsec).

	Complex				
	EN	AN	MN	PN	SN
${}^4G_{11/2}$	160	76	70	169	104
${}^2H_{9/2}$	572	412	415	637	480
${}^4F_{5/2}$	815	537	540	873	630
${}^4F_{7/2}$	536	404	404	601	455
${}^4S_{3/2}$	1597	772	812	1490	958
${}^4F_{9/2}$	1351	1276	1192	1658	1339
${}^4I_{9/2}$	6452	4274	4630	6993	5025
${}^4I_{11/2}$	23256	10870	11236	21277	13889
${}^4I_{13/2}$	18182	10417	11628	17241	12500

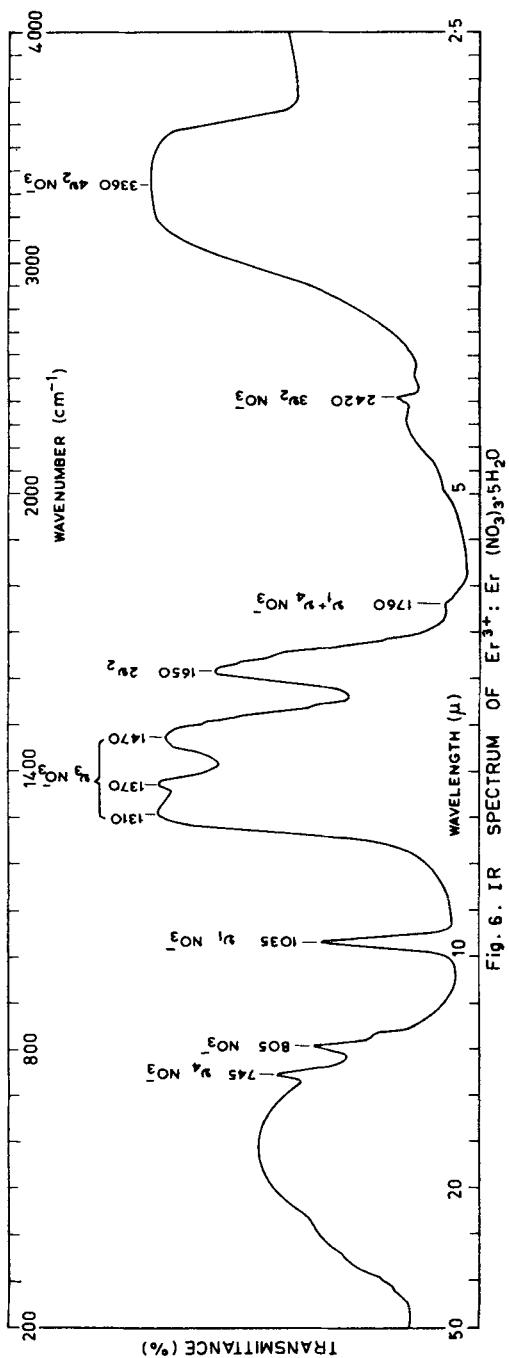


Figure 6. IR spectrum of $\text{Er}^{3+} : \text{Er}(\text{NO}_3)_3 \cdot 5\text{H}_2\text{O}$.

Table 5. Term assignments for components of broad bands resolved in the second derivative spectrum of Er^{3+} : EN.

Term	Band positions (cm^{-1})		
	Observed		
	Normal	Second derivative	Calculated*
$^2P_{3/2}$		31380	31703
$^2K_{13/2}$		31818	33042
$^4G_{5/2}$		32734	33374
$^4G_{7/2}$	33000	33539	34022
$^2D_{5/2}$		34269	34427
$^4G_{9/2}$		36602	36578
$^4D_{5/2}$		37476	38655
$^2I_{11/2}$		40052	40982
$^2L_{17/2}$	42000	41352	41473
$^2D_{3/2}$		42385	42098
$^4D_{3/2}$		43103	43000

* The wide deviations between observed and calculated values in some cases may be due to the use of spectroscopic parameters (E^k , etc.,) obtained from low energy bands.

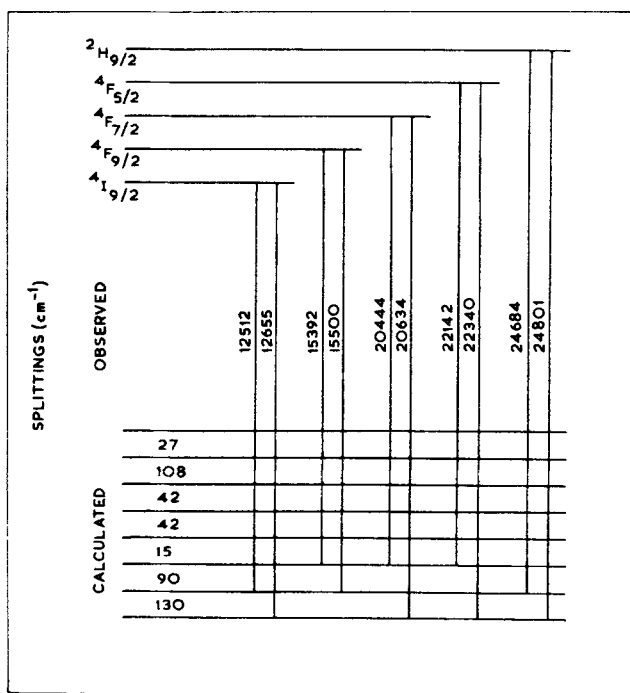


Figure 7. Energy level diagram showing observed transitions and calculated splittings for Er^{3+} in EN.

Table 6. Observed and calculated crystal field splittings of Er^{3+} complexes in cubic symmetry assumption (values in cm^{-1}).

	EN		AN		MN		PN		SN						
	OBS.	CAL.	OBS.	CAL.	OBS.	CAL.	OBS.	CAL.	OBS.	CAL.					
${}^2\text{H}_{9/2}$	[117]	130	[135]	145	[154]	156						
${}^4\text{F}_{5/2}$	[198]	220	[237]	215	[247]	219	[238]	229	[248]	235
${}^4\text{F}_{7/2}$	[190]	220	[199]	215	[190]	219	[220]	229	[221]	235
${}^4\text{F}_{9/2}$	[108]	90												
${}^4\text{I}_{9/2}$	[143]	130	[151]	145	[159]	156	[138]	138	[153]	153

Hufner 1978). The vibrational modes due to NO_3^- radical (Herzberg 1954) are also indicated in the IR spectra shown in figure 6. The third possibility may also be ruled out since the observed splittings in the second derivative are in no way comparable with the observed IR frequencies of figure 6.

In view of the limited IR data reported in literature and since the authors do not have access to far IR (below 200 cm^{-1}) instruments, the observed splittings are tentatively assumed to be due to a crystal field. The analysis presented is approximate and purely tentative.

The observed splittings are analysed by assuming cubic symmetry as detailed in our recent paper (Lakshman and Jayasankar 1984). The operator equivalent factors (β_j and γ_j) for the ground state (${}^4\text{I}_{15/2}$) of Er^{3+} ion in different complexes have been evaluated and presented in table 2 along with the crystal field parameters (A_{40} and A_{60}) following Lakshman and Jayasankar (1984). The energy level diagram showing the observed transitions and the calculated spacings is shown in figure 7 for Er^{3+} in EN. The final results showing the observed and calculated splittings are presented in table 6.

Acknowledgements

One of the authors (CKJ) thanks DST and CSIR (India) for award of fellowships.

References

- Carnall W T 1979 *Handbook on the physics and chemistry of rare earths* (New York: North Holland) Vol 3
 Carnall W T, Fields P R and Rajnak K 1968 *J. Chem. Phys.* **49** 4424

- Carnall W T, Fields P R and Wybourne B G 1965 *J. Chem. Phys.* **42** 3797
- Chang N C, Gruber J B, Leavitt R P and Morrison C A 1982 *J. Chem. Phys.* **76** 3877
- Crosswhite H M and Moos H W 1967 *Optical properties of ions in crystals* (New York: Interscience)
- Dieke G H 1968 *Spectra and energy levels of rare earth ions in crystals* (New York: Interscience)
- Faulkner T R, Morley J P, Richardson F S and Schwartz R W 1980 *Mol. Phys.* **40** 1481
- Gruber J B, Chirico R D and Westrum Jr. E F 1982 *J. Chem. Phys.* **76** 4600
- Hayhurst T, Shalimoff G, Edelstein N, Boatner L A and Abraham M M 1981 *J. Chem. Phys.* **74** 5449
- Herzberg G 1954 *Molecular spectra and molecular structure II, infrared and Raman spectra of polyatomic molecules* (New York: D. Van Nostrand)
- Hoogschagen J and Gorter C J 1948 *Physica* **14** 197
- Hufner S 1978 *Optical Spectra of transparent rare earth compounds* (New York: Academic Press)
- Koningstein J A and Geusic J E 1964 *Phys. Rev.* **136** A726
- Krupke W F and Gruber J B 1963 *J. Chem. Phys.* **39** 1024
- Lakshman S V J and Jayasankar C K 1984 *Spectrochimica Acta*
- Mazurak Z, Hanuza J, Hermanowicz K, Jezowska-Trzebiatowska B, Schultze D and Waligora Ch 1983 *J. Chem. Phys.* **79** 255
- Pappalardo R 1963 *Z. Phys.* **173** 374
- Peacock R D 1975 *Struct. Bonding* **22** 83
- Prandtl W and Scheiner K 1934 *Zeit. Anorg. Allgem. Chem.* **220** 107
- Reisfeld R 1975 *Struct. Bonding* **22** 123
- Reisfeld R and Eckstein Y 1975 *J. Chem. Phys.* **63** 4001
- Ryba-Romanowski W, Mazurak Z, Jezowska-Trzebiatowska B, Schultze D and Waligora Ch 1980 *Phys. Status Solidi* **A62** 75
- Stein G and Wurzberg E 1975 *J. Chem. Phys.* **62** 208
- Wong E Y 1961 *J. Chem. Phys.* **35** 544
- Wybourne B G 1965 *Spectroscopic properties of rare earths* (New York: Interscience)